

Article

Optimal Plastic Reliable Design of Reinforced Concrete Beams Considering Steel Bars Volume Probability

Sarah Khaleel Ibrahim and Majid Movahedi Rad * 

Department of Structural and Geotechnical Engineering, Széchenyi István University, 9026 Győr, Hungary

* Correspondence: majidmr@sze.hu

Abstract: This paper aims to investigate the plastic response of reinforced concrete tapered beams when subjected to random steel reinforcement volumes, using both deterministic and probabilistic analyses, with the complementary strain energy as a boundary in the first case, and the reliability index as a boundary in the second. The first step in this study was to use a previously studied model and perform a deterministic analysis, assuming that the complementary strain energy is a limiting factor and controller of the plastic behaviour. Next, a probabilistic analysis is applied, with the reliability index as a limitation. At the same time, the volume of the reinforcement steel used, and the complementary strain energy were treated as probabilistic variables with mean values and specific standard deviations. This novel method highlighted the plastic behaviour limiting procedure and provided results that highlighted the nature of the model's changed behaviour when the complementary strain energy was controlled and when applying probabilistic properties with reliability index limitation.

Keywords: optimal solution; plastic behaviour; steel volume; complementary strain energy; deterministic analysis; probabilistic analysis; reliability index

MSC: 65K10



Citation: Ibrahim, S.K.; Rad, M.M. Optimal Plastic Reliable Design of Reinforced Concrete Beams Considering Steel Bars Volume Probability. *Mathematics* **2023**, *11*, 2349. <https://doi.org/10.3390/math11102349>

Academic Editor: Gaohui Wang

Received: 2 April 2023

Revised: 14 May 2023

Accepted: 16 May 2023

Published: 18 May 2023



Copyright: © 2023 by the authors. Licensee MDPI, Basel, Switzerland. This article is an open access article distributed under the terms and conditions of the Creative Commons Attribution (CC BY) license (<https://creativecommons.org/licenses/by/4.0/>).

1. Introduction

Concrete is commonly classified as a brittle material due to its tendency to crack when subjected to tensile stresses. However, it is not entirely brittle as its tensile strength is considerably lower than its compressive strength, typically about one-tenth. Therefore, concrete is often referred to as a semi-brittle material, meaning it exhibits both brittle and ductile properties under different loading conditions. The presence of reinforcing materials, such as steel bars, can enhance the tensile strength of concrete and make it more ductile. Its tensile strength and its tensile toughness must be considered when analysing its cracking behaviour. The failure and fracture growth in concrete beams were examined by Sowik [1], who based his analysis on experimental study and numerical simulations. To learn more about how strain softening of tensile concrete develops in plain concrete and mildly reinforced concrete beams, a nonlinear fracture mechanics-based, fictional crack model was used. Results from the study show that the mechanism of failure in flexural beams changes depending on the longitudinal reinforcement ratio. In plain and lightly reinforced concrete beams, brittle failure occurs due to a flexural crack formation. Ashour [2] examined how the concrete compressive strength and flexural tensile reinforcement ratio affected the load-deflection behaviour and displacement ductility of cracked rectangular reinforced concrete beams by conducting a series of tests on nine reinforced high-strength concrete beams. A higher compressive strength of concrete is correlated with higher flexural rigidity. Furthermore, the effective moment of inertia changes from an uncracked portion to a fully cracked section based on the flexural tensile reinforcement ratio. In order to investigate how steel fibre content, longitudinal tensile

reinforcement ratio, and concrete compressive strength affect the flexural behaviour of reinforced concrete beams, Ashour et al. [3] evaluated twenty-seven beams. The results demonstrate that the tensile reinforcement ratio did not affect the additional moment strength given by the fibres. However, concrete compressive strength had a substantial impact on the fibre contribution. Mohammadhassani et al. [4] developed six full-scale reinforced HSC beams using the ACI code provisions, and cast them with compressive strengths ranging from 65 MPa to 75 MPa, and then tested them under two-point top loading. An increase in the tensile reinforcement ratio causes a rise in the number of cracks, while their depth and width decrease with the ratio. Reinforced HSC beams behave elastically, and the tensile reinforcement ratio increases the ultimate load.

The ever-increasing need for cost-effective buildings has piqued the attention of design professionals eager to improve methods for the optimal design of structural components. The optimisation aspect of structural design is not heavily covered by the codes and instead relies heavily on the designer's prior expertise, which cannot replace the tried-and-true principles of optimisation methods. The optimal design of reinforced concrete beams for various design conditions was described by Chakrabarty [5], who also explained the design economics, cost function, and modelling involved. Depending on the unit cost of the materials and shuttering, the beam dimensions, and the reinforcement ratio, the cost of a beam might vary significantly. Since many different beam dimensions and reinforcement ratios exist that provide the exact moment of resistance, it becomes challenging to accomplish the least-cost design using traditional approaches. With material and shuttering costs, as well as structural constraints taken into account, this work proposes a geometric programming model that yields the optimal least-cost design of a beam.

In addition, experimental results on the load-deflection relationship of six simply supported reinforced concrete beams with varying rates of longitudinal reinforcement were published by Mansor et al. [6]. The results show that the ductility index drops dramatically with an increase in the reinforcement ratio for low reinforcement values. This, however, is mitigated when the reinforcement ratio increases. Lep et al. [7] described how a class of optimisation issues connected to the design of steel-reinforced concrete structures might be approached using strategies based on genetic algorithms. The primary goal of this design was to reduce the building's overall price cost. The final structure must meet all strength and serviceability requirements for the imposed load level, but it must also be priced competitively. Solving a problem of this complexity with this many restrictions requires an optimisation method that is both fast and dependable. In this case, the problem was solved using the augmented simulated annealing technique. The application of the proposed method is evaluated by analysing a plain continuous steel reinforced beam. Chutani and Singh [8] introduced a standard optimisation method, Particle Swarm Optimisation (PSO), for the optimal design of RC beams. Cost savings are achieved through the appropriate cross-sectional dimensions of an RC beam; however, this cannot be standardised due to the many elements that affect each given design. In order to optimise the reinforced concrete beams after the removal of the supports, Tamrazyan and Alekseytsev [9] devised an algorithm based on an altered genetic algorithm and RBDO strategy. Elements can have a wide range of cross-sectional sizes and variations in the concrete type, reinforcement type, and reinforcement diameter. The primary active constraints seek to keep the structure's geometry as unaltered as possible following emergency interventions.

By using the novel formulation provided by Guerra and Kiouisis [10] for the optimal design of RC structures, beam and column elements in multi-bay and multi-story buildings could be optimally sized and reinforced to keep ahead of optimal stiffness correlations between all structural components while economising. Lastly, the literature on optimising reinforced concrete (RC) beams has been summed up by Rahmanian et al. [11]. Different optimisation methods have been used to provide the optimal design of RC beams, either as standalone structural components or as part of a structural frame, due to differences in the objective of optimisation (e.g., minimum cost or weight), the design variables, and the constraints considered by different studies. Given the limited design parameters, the

literature survey indicates that nonlinear deterministic techniques can be used effectively to provide an optimal design of RC beams.

With the complementary strain energy of residual forces created inside the steel reinforcing bars, Rad et al. [12] introduced a unique computational model to regulate the plastic behaviour of reinforced concrete haunched beams. Different objective functions were considered while applying the optimal elasto-plastic analysis and design of haunched reinforced concrete beams to find the maximum loading or the minimum volume of the steel used to reinforce the beams as constraints on the complementary strain energy of the residual internal forces of the steel bars that regulate the plastic deformations. This research builds on previous work in this area [12] by considering both a deterministic and a probabilistic scenario. The complementary strain energy is taken as the limit of the plastic behaviour and works as a limiting index in the deterministic situation. On the other hand, the reinforcement volume and complementary strain energy will be counted as probabilistic values in a reliability-based design defining the probabilistic scenarios. A deterministic solution was obtained by initiating the numerical model in ABAQUS with the concrete damage plasticity model (CDP) and calibrating it against experimental results, then applying the plastic behaviour limitation principle by using a novel code written by the authors while considering the constant value for the complementary strain energy (W_{p0}). The number of yielding elements inside the steel bars determines the complementary strain energy value (W_p), which is, in turn, computed from the number of residual stresses within the bars. Then, we investigated reinforced concrete beams with random steel volumes and allowable complementary strain energy W_{p0} values to examine how the uncertainty of these variables would affect the beams' overall behaviour. This unpredictability reflects the inevitable randomization of reinforcing bar diameters that occurs during construction due to uncontrollable human error. The outcomes are presented so that the impact of such errors on the behaviour of the structural parts may be comprehended and taken into account. Furthermore, the complementary strain energy would be a limit to avoid plastic and post-plastic behaviour throughout any structure's lifetime by fixing the most secure W_{p0} value to keep the behaviour inside the elastic-plastic region (or pre-plastic region) where the complementary strain energy classifies the structure behaviour into elastic, elastic-plastic and plastic depending on the load values as shown in Figure 1.

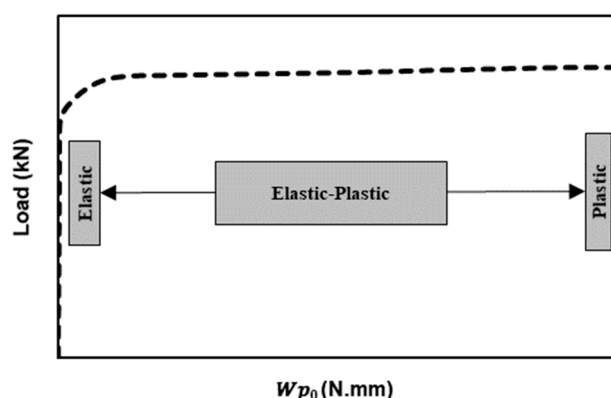


Figure 1. Complementary strain energy effect on a structure [12].

Thus, the research described builds on previous work in the same area. Specifically, the previous study by Rad et al. [12] introduced a computational model that used the complementary strain energy of residual forces in steel reinforcing bars to regulate the plastic behaviour of reinforced concrete haunched beams. Different objective functions were considered, and optimal elasto-plastic analysis and design were applied to find the maximum loading or minimum volume of steel used to reinforce the beams while ensuring that the complementary strain energy of residual internal forces of the steel bars regulated the plastic deformations.

In this current study, we considered both deterministic and probabilistic scenarios for the same problem. In the deterministic scenario, the complementary strain energy was taken as the limit of plastic behaviour and used as a limiting index considering more detailed and novel termination values. The reinforcement volume and complementary strain energy were treated as probabilistic values in a reliability-based design in the probabilistic scenario to examine how the uncertainty of these variables would affect the beams' overall behaviour.

This probabilistic process was presented for both steel volume and complementary strain energy of the internal stresses, knowing that dealing with the complementary strain energy value as a random value is considered a novel work. This approach is significant because the complementary strain energy value is a critical parameter that regulates the plastic behaviour of the beams. By considering it as a random variable, we were able to account for the inevitable randomization of reinforcing bar diameters that occurs during construction due to uncontrollable human error.

The probabilistic approach allowed for the examination of a range of possible outcomes based on different combinations of steel volume and complementary strain energy values. This information can be used to better understand the behaviour of the structural components and to optimise the design process.

Following this introduction, the methodology used in this study is presented in Section 2. Then, the details of the modelled beams are found in Section 3, while Sections 4 and 5 contain the discussion of the obtained results and the most important conclusions, respectively.

2. Approaches and Principals

2.1. Principle of Plasticity-Based Behaviour Restriction

This technique is employed in plastic analysis and design. It accounts for residual stresses by utilising complementary strain energy, which has been effectively applied to various structures [13–16]. To account for the strain energy of residual forces as a thorough evaluation of plastic behaviour, a suitable computational technique was devised for use where such energy quantity limits are required to govern residual deformations. Here we present the residual forces responsible for creating this additional strain energy:

$$W_p = \frac{1}{2E} \sum_{i=1}^n \frac{l_i}{A_i} N_i^{R2} \leq W_{p0}. \quad (1)$$

The greatest elastic strain energy that can be used to determine W_p for a given structure is defined here by W_{p0} [14]. The Young's modulus of the bar material is defined by E , the residual force of the bar members is defined by N_i^R , the length of the bar elements is defined by l_i , ($i = 1, 2, \dots, n$), the cross-sectional area of the bar elements is identified by A_i , ($i = 1, 2, \dots, n$), and so on. A limit value W_{p0} is introduced for plastic rebar deformations in Equation (1). The residual forces NR that are visible in the structure upon unloading are represented by the inner plastic force N^{pl} —which will occur when the load P_0 is applied—and the internal elastic force— N^{el} .

$$N^R = N^{pl} - N^{el} \quad (2)$$

Knowing that, N^{el} represents the elastic force acting on a physical object:

$$N^{el} = F^{-1}G^TK^{-1}P_0. \quad (3)$$

Matrix F stands for adaptability, while Matrix G represents geometry, but Matrix K defines the stiffness. Taken together, this equation represents a way to calculate the elastic force acting on a physical object based on information about its initial state (P_0) and the properties of its material (represented by matrices F , G , and K). In particular, the equation involves taking the inverse of matrices F and K , transposing matrix G , and then performing

a series of matrix multiplications to obtain the final result for elastic force acting on a physical object N^{el} .

2.2. Theory of Probabilities

Theoretically, we expect $f_R(X_R)$ and $f_S(X_S)$ to be the probability density functions of X_R and X_S , respectively, for the case where $X_R \leq X_S$. The following equation, presented by Murzewski [17], provides a calculation of the failure probability:

$$P_f = P[X_R \leq X_S] = \iint_{X_R \leq X_S} f_R(X_R) f_S(X_S) dX_R dX_S. \quad (4)$$

Using the well-known bound state function, which is defined as:

$$g(X_R, X_S) = X_R - X_S. \quad (5)$$

The failure domain, D_f , is represented by the value $g \leq 0$. In the context of a mathematical optimisation problem, D_f represents the domain of the objective function. This means that D_f is the set of input values that can be used as arguments for the objective function. In this case, the value $g \leq 0$ is used to represent the domain of the function because it is a constraint that must be satisfied for the problem to be feasible.

Therefore, we can write down the failure probability P_f :

$$P_f = F_g(0). \quad (6)$$

In addition, P_f can be assumed by [17]:

$$P_f = \int_{g(X_R, X_S) \leq 0} f(X) dX = \int_{D_f} f(X) dX. \quad (7)$$

In this investigation, we place bounds on the complementary strain energy of the residual forces using a Gaussian distribution with a mean of \bar{W}_{p0} and a standard deviation of σ_w , which accounts for the uncertainties in the data. The reliability index (β) is computed using the probability of failure (P_f) values and the Monte Carlo sampling technique. The probability density function $f_X(x)$ is generated as a random vector X , and realisations x are generated using the Monte Carlo method. The percentage of points (P_f) in the failure domain can be calculated by simply counting the total number of points. If we have a D_f , indicator function, we may write the following to express the idea.

$$\chi_{D_f}(x) = \begin{cases} 1 & \text{if } x \in D_f \\ 0 & \text{if } x \notin D_f \end{cases}. \quad (8)$$

By reshaping Equation (7):

$$P_f = \int_{-\infty}^{+\infty} \dots \int_{-\infty}^{+\infty} \chi_{D_f}(x) f_X(x) dx. \quad (9)$$

Since $\chi_{D_f}(X)$ stands for a randomly distributed two-point variable.

$$\mathbb{P}[\chi_{D_f}(X) = 1] = P_f. \quad (10)$$

$$\mathbb{P}[\chi_{D_f}(X) = 0] = 1 - P_f. \quad (11)$$

Here, $P_f = \mathbb{P}[X \in D_f]$.

To determine the mean and standard deviation of a random variable $\chi_{D_f}(X)$:

$$\mathbb{E}[\chi_{D_f}(X)] = 1 \cdot P_f + 0 \cdot (1 - P_f) = P_f \quad (12)$$

$$\mathbb{V}ar[\chi_{D_f}(X)] = \mathbb{E}[\chi_{D_f}^2(X)] - (\mathbb{E}[\chi_{D_f}(X)])^2 = P_f - P_f^2 = P_f(1 - P_f). \quad (13)$$

To assess P_f via the Monte Carlo technique, by means of the next formulation:

$$\hat{\mathbb{E}}[\chi_{D_f}(X)] = \frac{1}{Z} \sum_{z=1}^Z \chi_{D_f}(X^{(z)}) = \hat{P}_f. \quad (14)$$

For a collection of random vectors with $(z = 1, \dots, Z)$, it can be shown that $X^{(z)}$ is a demonstration, and that $f_X(x)$ is a function of (x) .

To emphasise, probabilistic models use the complementary strain energy as a random variable. We can therefore determine its average and standard deviation. Moreover, it follows the Gaussian distribution: mean is \mathbb{E} , and variance is $\mathbb{V}ar$. The median and standard deviation of the estimator can be calculated using:

$$\mathbb{E}[\hat{P}_f] = \frac{1}{Z} \sum_{z=1}^Z \mathbb{E}[\chi_{D_f}(X^{(z)})] = \frac{1}{Z} Z P_f = P_f \quad (15)$$

$$\mathbb{V}ar[\hat{P}_f] = \frac{1}{Z^2} \sum_{z=1}^Z \mathbb{V}ar[\chi_{D_f}(X^{(z)})] = \frac{1}{Z^2} Z P_f (1 - P_f) = \frac{1}{Z} P_f (1 - P_f). \quad (16)$$

The reliability constraint, (β) [18,19], can be expressed as:

$$\beta_{target} - \beta_{calc} \leq 0 \quad (17)$$

where Equation (17) presents the optimisation termination condition to ensure that β_{calc} is less than β_{target} through the whole process until termination. At the end of each iteration, the reliability index is calculated as β_{calc} , and once β_{target} is reached, the procedure terminates. To calculate β_{target} and β_{calc} , we use the following notations:

$$\beta_{target} = -\Phi^{-1}(P_{f,target}). \quad (18)$$

$$\beta_{calc} = -\Phi^{-1}(P_{f,calc}) \quad (19)$$

As such, Φ^{-1} stands in for the truncated normal distribution, which is the inverse of the normal distribution function, setting a maximum value for the complementary strain energy, W_{p0} , the code interprets the reliability index as a limiting index that indicates when the problem has been solved, after which the correct load, deflection, and complementary strain energy are computed.

2.3. The Optimal Design Problem

This section focuses on creating the mathematical formula to specify the optimum reinforcement volume used in reinforced concrete haunched beams. To find the least amount of steel needed for the haunched beam (V), a nonlinear optimisation method is applied. It is optional to do incremental updates of the constitutive elements when using the extremum principles of plasticity. Additionally, A_i and l_i stand for each element's cross-sectional area and length, respectively [12].

$$\text{Min.} \rightarrow V = \sum_i A_i l_i \quad (20)$$

$$\text{Subjected to : } N^{el} = F^{-1} G K^{-1} P_0; \quad (21)$$

$$-N^{pl} \leq N^{pl} \leq N^{pl}; \quad (22)$$

$$\frac{1}{2E} \sum_{i=1}^n \frac{l_i}{A_i} N_i^{R2} \leq W_{p0}. \quad (23)$$

$$u - u_o < 0 \quad (24)$$

The first presented equation, Equation (20), defines the optimal steel volume problem where the lower and upper-plastic limit conditions are shown by Equation (22), where N^{pl} is the ultimate plastic limit load, and Equation (21) calculates the elastic fictitious internal regular forces. In addition, boundary Equation (23) depicts the complementary strain energy of residual forces utilised to control plastic deformations of steel bars as a global measure of the structure's plastic behaviour. Presenting u as the deflection value obtained through the optimisation and u_o as the maximum deflection value, Equation (24) illustrates the deflection condition. Providing the calculated value of the complementary strain energy of the residual forces is less than or equal to the boundary for the magnitude of the allowable complementary strain energy of the residual forces, the plastic deformations can be assumed to be under control, allowing for a deterministic solution. Once the corresponding strain energy W_{p0} is achieved, the solution is stopped.

In contrast, when investigating the probabilistic solution, we substitute Equation (17) $\beta_{target} - \beta_{calc} \leq 0$ for Equation (23), announcing that the termination condition is then governed by the probabilistic complementary strain energy, which is chosen at random for each iteration and subject to the appropriate mean value \bar{W}_{p0} and standard deviation σ_w . In cases when the estimated reliability index (β_{calc}) exceeds the permitted target value (β_{target}), the probabilistic solution would be abandoned. The study also considers the optimisation steps shown in Figure 2, where it is crucial to remember that the CDP parameters included in the optimisation issue are kept fixed throughout the analysis. While the deterministic phase applies these specifics, the probabilistic phase will consider utilising a 10% and 30% standard deviation on the complementary strain energy value and the steel volume, respectively.

To further elaborate on the optimisation process, the researchers modelled the beams using experimental results and calibrated the computational model using the concrete damage plasticity (CDP) model. The calibrated model was then used to perform an optimisation problem where the complementary strain energy of residual forces was set as the termination condition. The objective function of the optimisation problem was to minimize the steel reinforcement volume while keeping the complementary strain energy below a certain value.

After obtaining a deterministic solution, the researchers applied a probabilistic optimisation process with a variable steel volume value and complementary strain energy while the reliability index worked as the termination condition. The complementary strain energy and steel reinforcement volume were treated as random variables in this case, reflecting the uncertainty in the reinforcing bar diameter during construction. The probabilistic optimisation process allowed the researchers to investigate how the uncertainty of these variables would affect the behaviour of the haunched reinforced concrete beams.

The reliability index was used as the termination condition for the probabilistic optimisation process. If the estimated reliability index exceeded the target value, the probabilistic solution would be abandoned.

The Lagrange multiplier method was employed in this study, which incorporated a Lagrange multiplier into the objective function to handle constraints. The Lagrange multiplier method is a commonly used method of facing constraints in optimisation problems.

It involves introducing a Lagrange multiplier to the objective function to account for the constraints and adjust the solution accordingly.

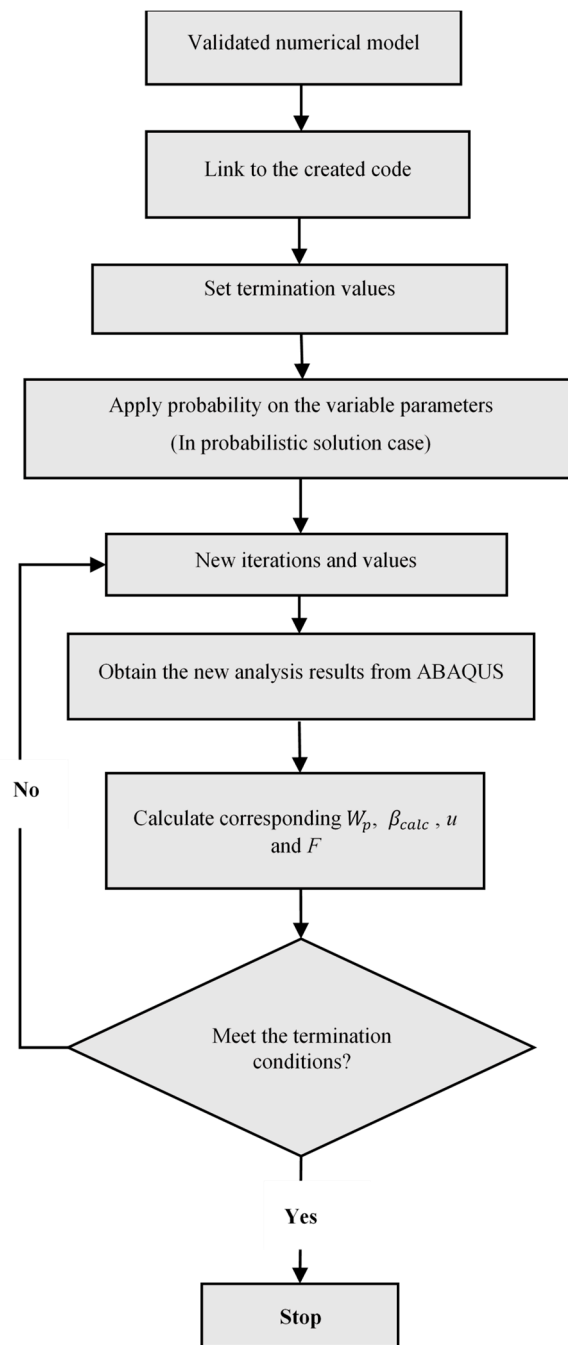


Figure 2. The considered optimisation steps.

3. Models Details

Recent research [12] considered the haunched beam model during assessment; in this case, model validation came first during optimisation; 3D finite element models were constructed based on experimental testing conducted in Széchenyi István University's lab. The CDP model was utilised to represent concrete within ABAQUS [19], and experimental findings from three simply supported haunched beams were used to validate the numerical model. Four samples were generated for the concrete material properties adoption tests, two for the compressive behaviour using the standard cube test and two for the tensile behaviour using the split-cylinder test. As this study concentrates on the steel part, Table 1

shows the characteristics of the steel utilised to reinforce the beams, while Figure 3 shows its distribution inside the studied beams.

Table 1. Characteristics of reinforcing steel.

Specifications	Yield Strength (MPa)	Ultimate Tensile Strength (MPa)	Elastic Modulus (MPa)
$\phi = 4 \text{ mm}$	550	626	210,000
$\phi = 8 \text{ mm}$	558	636	210,000
$\phi = 16 \text{ mm}$	489	556	210,000

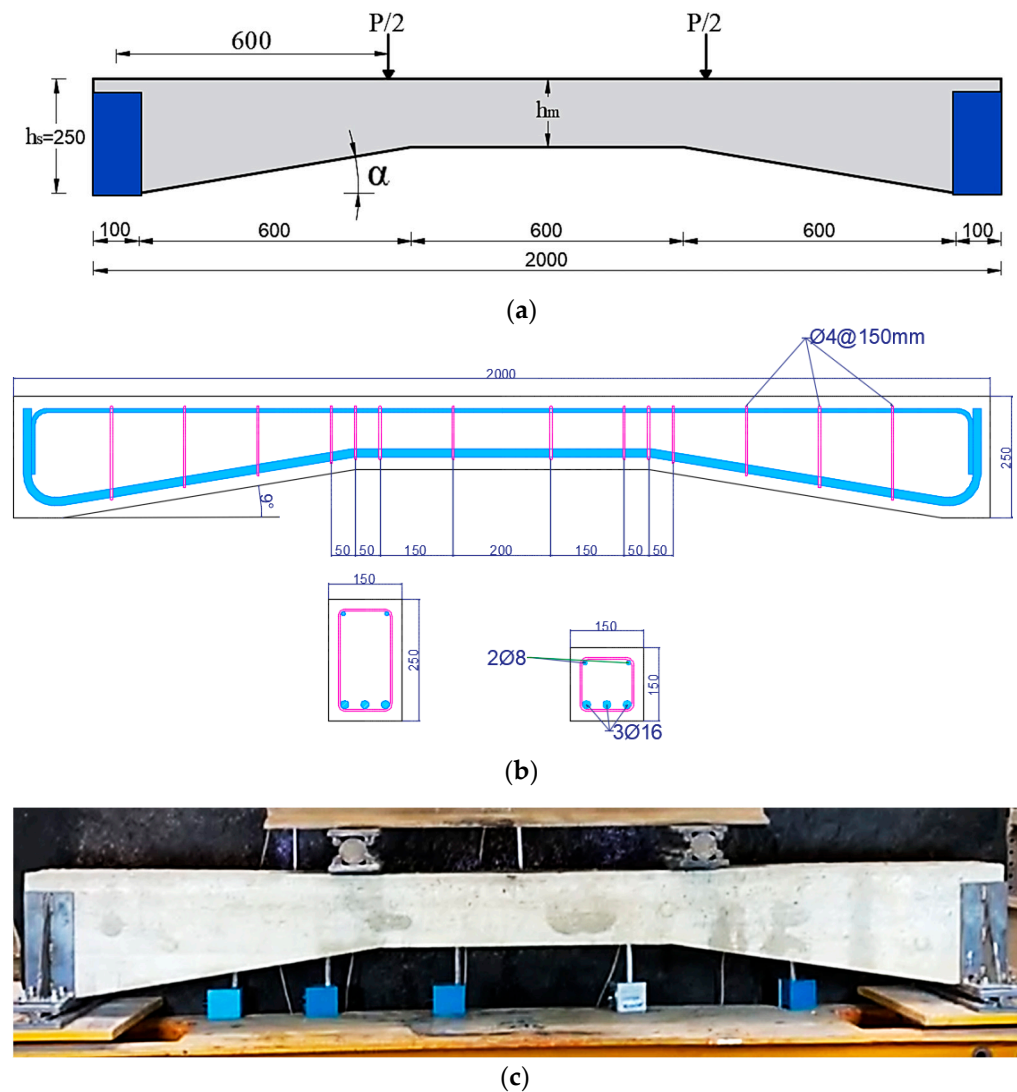


Figure 3. Details of the studied Beam: (a) Beam geometry, (b) Reinforcement details, (c) Experimental test setup.

The shear behaviour of haunched beams was determined through laboratory testing of beam specimens after two days of curing, looking at the cracking pattern, failure mode, and load-deflection relationship according to Rad et al. [12]. The beams measured a total of 2000 mm in length, with a constant cross-sectional area at the supports and a gradual drop toward the beam's mid-span, which resulted in a haunch angle (α) of 2 degrees as shown in Figure 3. Two concentrated monotonic loadings were applied to each beam until failure occurred during a series of tests; the resulting values were used to build the numerical model shown in Figure 4.

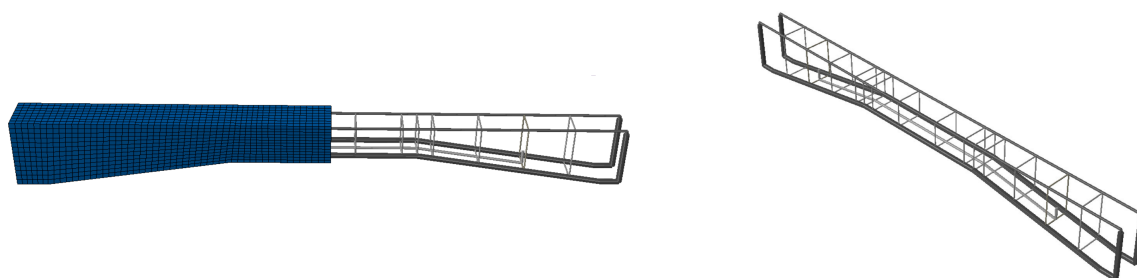


Figure 4. The numerically modelled beams.

Concrete and reinforcement bars were used to construct the finite element model; the former was represented by a solid element with eight nodes (C3D8: eight-node first-order hexahedral element with an exact numerical integration), while the latter were modelled as beam elements with a two-node linear beam in space (B31: Timoshenko beam). Concrete was poured into an embedded zone to simulate the link between longitudinal and transverse reinforcements. The nonlinear behaviour of the haunched beams was modelled using finite element failure analysis using a damage plasticity approach [20,21]. The mechanical properties test of specimens causes concrete damage plasticity data, including compressive crushing and tensile cracking as failure mechanisms of the material; these properties are inserted into ABAQUS to obtain CDP parameters that reflect the required damage behaviour of concrete. To ensure that the results were comparable to those obtained in the lab, the boundary conditions were set accordingly. Furthermore, in order to replicate the experimental conditions, a concentrated vertical load was supplied at each point load of the beam, and the coupling effect was used to disperse the loads evenly. Both numerical accuracy and computation time can be affected by the mesh size, so a size study was performed to see how different mesh sizes performed. Subsequently, an optimal mesh size was used to get a precise result, with a total element count of the beams equalling around 9500.

4. Results and Discussions

This section presents the optimisation process considering two different scenarios. The first scenario involves a deterministic solution where the steel volume remains constant throughout the optimisation process. The results of this scenario are illustrated in the first three rows of Table 2. Three different allowable complementary strain energy values were chosen as termination conditions ($W_{p0} = 335, 95, 25 \text{ Nmm}$); these values were considered to understand the effect of having limited complementary strain energy values on the behaviour of the beams and load and deflection values. As previously explained in Section 2, the complementary strain energy is defined primarily by the amount of yielded parts inside steel bars; these parts increase as the load increases; usually, the steel starts to yield after the concrete cracks and tension fails, and then the cracks extend from supporting to reach the loading points, revealing that the beam is no longer capable of handling any extra stress. Then, the rule is transferred to the steel bars to handle the extra incoming stress until the total failure of the structure occurs; this behaviour can be observed in most load-deflection relationships (curves) of concrete structures, where the start of these curves gives an almost short straight line revealing a brief period of elasticity where no plastic deformation nor yielded elements are found, and therefore W_p is zero at this stage. The elastic-plastic region is present where the plasticity begins and W_p starts to have small values reflecting the presence of yielded steel elements. Finally, at the prior peak of the curve where the failure is about to occur, W_p has its highest values, reflecting high plastic damage intensity inside the steel bars and the beam in general. Results shown in Table 2 (cases 1–3) prove the effectiveness of W_p to control the plastic behaviour [22,23], where it can be seen that higher W_{p0} values give higher load and deflection values meaning the model undergoes higher stresses, and so more damage is shown. Likewise, Table 3 shows the damage intensity for these cases in both concrete and steel, as the red areas represent the fully damaged parts. In contrast, the blue areas represent the undamaged parts. In case

three, when W_{p0} is at its minimum, the damage inside the concrete and steel is minor if compared to the other cases.

Table 2. Results obtained for deterministic and probabilistic cases.

	Case No.	W_{p0} (Nmm)	β_{target}	V (mm)	F (kN)	u (mm)
Deterministic	1	335	-	140×108	62.5	18.3
	2	95			51	10.3
	3	25			37	6
Probabilistic	4	Randomly	3.1	Randomly	95	17
	5	changed by	3.5	changed	82	15
	6	10%	4.8	by 30%	79	14

Table 3. Damage representation for deterministic and probabilistic cases.

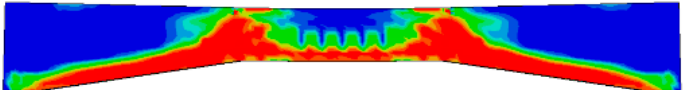
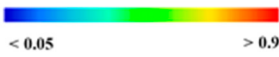


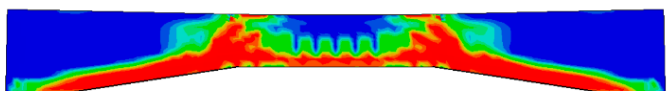

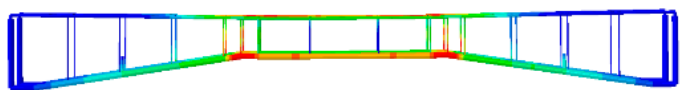
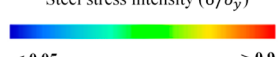
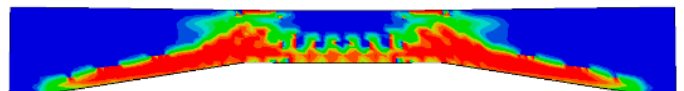
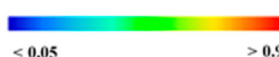
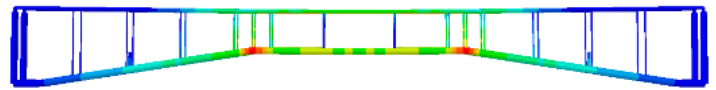

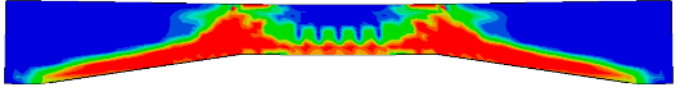

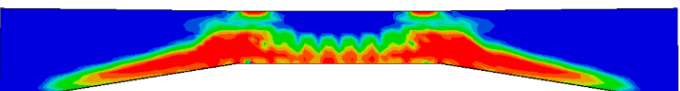
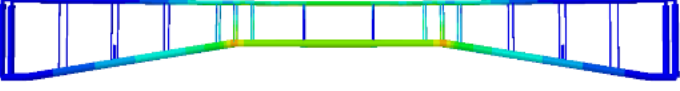
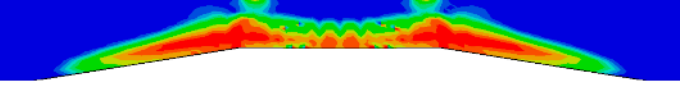

Case	Material	Damage Pattern
1	Concrete	 <p>Tension damage coefficient (d_t)</p>  <p>< 0.05 > 0.9</p>
	Steel	 <p>Steel stress intensity (σ/σ_y)</p>  <p>< 0.05 > 0.9</p>
2	Concrete	 <p>Tension damage coefficient (d_t)</p>  <p>< 0.05 > 0.9</p>
	Steel	 <p>Steel stress intensity (σ/σ_y)</p>  <p>< 0.05 > 0.9</p>
3	Concrete	 <p>Tension damage coefficient (d_t)</p>  <p>< 0.05 > 0.9</p>
	Steel	 <p>Steel stress intensity (σ/σ_y)</p>  <p>< 0.05 > 0.9</p>

Table 3. Cont.

Case	Material	Damage Pattern
4	Concrete	 <p>Tension damage coefficient (d_t)</p> <p>< 0.05 > 0.9</p>
	Steel	 <p>Steel stress intensity (σ/σ_y)</p> <p>< 0.05 > 0.9</p>
5	Concrete	 <p>Tension damage coefficient (d_t)</p> <p>< 0.05 > 0.9</p>
	Steel	 <p>Steel stress intensity (σ/σ_y)</p> <p>< 0.05 > 0.9</p>
6	Concrete	 <p>Tension damage coefficient (d_t)</p> <p>< 0.05 > 0.9</p>
	Steel	 <p>Steel stress intensity (σ/σ_y)</p> <p>< 0.05 > 0.9</p>

Furthermore, the second scenario, represented by cases 4–6, deals with the effect of random steel volumes used to reinforce the haunched beams, as the diameters of the bars used in the presented model were changed randomly within a 30% standard deviation of the volume mean value ($140 \times 108 \text{ mm}^3$), and the allowable complementary strain energy value is considered a probabilistic value as well, by taking 335 Nmm as the mean value and having a standard deviation of 10%. These values were considered after applying the appropriate sensitivity test to understand which changing percentages had a noticeable effect on the results. In addition, the reliability index is taken into account in this probabilistic scenario as a limitation index with three chosen values ($\beta_{target} = 3.1, 3.5, 4.8$). These values were chosen following the Eurocode [24] specifications for the permissible values. Tables 2 and 3 provide the results, which show both scenarios. Table 3 shows that the decreasing reliability index reflects the increased damage severity where it can be seen the concrete damage is represented by the tension damage coefficient (d_t) extracted by ABAQUS, while the steel

stress severity is given by σ/σ_y . It can be seen that for the three first cases, higher damaged areas (red parts) are obtained in steel bars as the complementary strain energy is increased. On the other hand, regarding the probabilistic cases, the damaged parts are changing as it is affected by the random complementary strain energy values and steel volume and a higher reliability index value is reflected in less steel damage inside the models.

In summary, this method was applied to eliminate errors resulting from inaccurate steel manufacturing processes or any error caused by humans during the construction process, as the diameters of steel bars used for reinforcement in reinforced concrete structures may not have the accuracy prescribed, and here the effect of errors and uncertainty on the behaviour of the elements is studied. In addition, it has been taken into consideration that there is a random probability of the allowable complementary strain energy to note the effect of its random change on the studied elements. It can be seen from Table 2 that the probability and change in variable values have an apparent effect on the values of the load and the resulting deformation in cases 4–6. The values of the reliability coefficient were chosen with values higher than three and on three different values to be the limit at which the analysis stops; thus, it has worked as a constraint that stops the progress of the stresses, where it is clear that the higher the value of this coefficient, the results will give the impression that the elements are far from failure and the plastic deformation and behaviour is less present. Therefore, it is considered a more reliable solution if we compare it with cases with a lower reliability coefficient, as shown in Table 3, which shows the severity of the damage within steel and concrete for these different cases; the damage is represented by a gradation of colours from red, i.e., complete damage, to blue, i.e., the absence of damage.

The time required to solve a deterministic steel volume optimisation problem can vary greatly based on factors such as problem complexity, model size, and computational resources. For simple problems, it may take only a few seconds to a few minutes, while more complex problems could require several hours or even days. In this study, the normal optimisation process took approximately 5500 s.

In contrast, solving a probabilistic optimisation problem generally requires more time than solving a deterministic optimisation problem due to the need for multiple simulations or evaluations to account for uncertainty and variability in the input parameters. Therefore, the time required to solve a probabilistic optimisation problem may range from several hours to days or even weeks for a mid-range complexity problem.

5. Conclusions

According to a recent study, this study examines deterministic and probabilistic scenarios [12]. The complementary strain energy limits plastic behaviour and acts as a limiting index in deterministic situations. In a reliability-based design that defines probabilistic situations, reinforcing volume and complementary strain energy are probabilistic parameters. A deterministic solution was obtained by starting the numerical model in ABAQUS, applying the plastic behaviour limitation principle, and considering the constant value for the complementary strain energy (W_{p0}). The complementary strain energy value (W_p) of steel bars is calculated from their residual stresses and yielding elements. Reinforced concrete beams with random steel volumes and permissible complementary strain energy W_{p0} values are studied to see how uncertainty affects their behaviour. Due to human error, reinforcing bar widths randomly vary during construction. The results show how such errors affect structural elements. The complementary strain energy limits plastic and post-plastic behaviour throughout a structure's lifetime by fixing the safest W_{p0} value to keep the behaviour in the elastic-plastic region (or pre-plastic region).

Generally, higher allowable complementary strain energy values are associated with larger load and deflection values, indicating that the structure is subjected to greater stresses and suffers greater damage as a result. However, when the allowable complementary strain energy is low, there is far less internal damage to the concrete and steel than in the other cases. Moreover, in the probabilistic solution, the reliability index functions as a constraint that suspends the progress of stresses; it is evident that the higher the value of

this coefficient, the more the results appear to indicate that the elements are far from failure and that the plastic deformation and behaviour are minimal. Consequently, compared to scenarios with a lower reliability coefficient, this solution is regarded as more reliable.

This theory was applied in this research, and the results proved that it is an effective method to find the optimal solution by controlling the plastic behaviour of the studied elements. It is worth noting that this method can be applied in future research, taking into account the possibility of different characteristics other than reinforcement steel volume or choosing different structural elements under various test conditions, such as the application of the effect of heat or the application of dynamic loads, such as build up capacity domains by using the method described by Sessa et al. [25].

The scalability of the provided methodology to practical engineering challenges of bigger scales may be limited by computational complexity as the process uses Monte Carlo simulation, which can be computationally intensive and time-consuming for larger tasks. This can significantly increase optimisation time and limit the method's practicality. In addition, the methodology may not work for highly complicated structural systems with many input parameters and sophisticated analyses.

The methodology's scalability to bigger practical engineering challenges may be limited. However, as the method discussed is a Monte Carlo simulation to develop dependable structural parts, the technique accounts for element behaviour mistakes and uncertainty caused by faulty steel manufacturing procedures or building errors and multiple simulations or evaluations accounting for input parameter stochasticity and unpredictability. The results determine the probability and effect of factors on load and structure deformation which prevents failure and plastic deformation.

Author Contributions: Conceptualization, methodology and investigation were performed by S.K.I. and M.M.R.; writing—original draft preparation, S.K.I.; supervision, M.M.R.; all authors were involved in the final editing. All authors have read and agreed to the published version of the manuscript.

Funding: This research received no external funding.

Data Availability Statement: The datasets, which were generated and analysed during the current study are available in the main manuscript, any additional details can be obtained from the Authors.

Conflicts of Interest: The authors declare that they have no known competing financial interest or personal relationships that could have appeared to influence the work reported in this paper.

References

1. Słowik, M. The analysis of failure in concrete and reinforced concrete beams with different reinforcement ratio. *Arch. Appl. Mech.* **2019**, *89*, 885–895. [\[CrossRef\]](#)
2. Ashour, S.A. Effect of compressive strength and tensile reinforcement ratio on flexural behavior of high-strength concrete beams. *Eng. Struct.* **2000**, *22*, 413–423. [\[CrossRef\]](#)
3. Ashour, S.A.; Wafa, F.F.; Kamal, M.I. Effect of the concrete compressive strength and tensile reinforcement ratio on the flexural behavior of fibrous concrete beams. *Eng. Struct.* **2000**, *22*, 1145–1158. [\[CrossRef\]](#)
4. Mohammadhassani, M.; Akib, S.; Shariati, M.; Suhatri, M.; Khanouki, M.A. An experimental study on the failure modes of high strength concrete beams with particular references to variation of the tensile reinforcement ratio. *Eng. Fail. Anal.* **2014**, *41*, 73–80. [\[CrossRef\]](#)
5. Chakrabarty, B. Models for optimal design of reinforced concrete beams. *Comput. Struct.* **1992**, *42*, 447–451. [\[CrossRef\]](#)
6. Mansor, A.A.; Mohammed, A.S.; Salman, W.D. Effect of longitudinal steel reinforcement ratio on deflection and ductility in reinforced concrete beams. In *IOP Conference Series: Materials Science and Engineering*; IOP Publishing: Bristol, UK, 2020; Volume 888, p. 012008. [\[CrossRef\]](#)
7. Lepš, M.; Šejnoha, M. New approach to optimization of reinforced concrete beams. *Comput. Struct.* **2003**, *81*, 1957–1966. [\[CrossRef\]](#)
8. Chutani, S.; Singh, J. Design Optimization of Reinforced Concrete Beams. *J. Inst. Eng. Ser. A* **2017**, *98*, 429–435. [\[CrossRef\]](#)
9. Tamrazyan, A.; Alekseytsev, A. Evolutionary optimization of reinforced concrete beams, taking into account design reliability, safety and risks during the emergency loss of supports. In *E3S Web of Conferences*; EDP Sciences: Les Ulis, France, 2019; Volume 97, p. 04005. [\[CrossRef\]](#)
10. Guerra, A.; Kioussis, P.D. Design optimization of reinforced concrete structures. *Comput. Concr.* **2006**, *3*, 313–334. [\[CrossRef\]](#)

11. Rahmanian, I.; Lucet, Y.; Tesfamariam, S. Optimal design of reinforced concrete beams: A review. *Comput. Concr.* **2014**, *13*, 457–482. [[CrossRef](#)]
12. Rad, M.M.; Ibrahim, S.K.; Lógó, J. Limit design of reinforced concrete haunched beams by the control of the residual plastic deformation. In *Structures*; Elsevier: Amsterdam, The Netherlands, 2022; Volume 39, pp. 987–996. [[CrossRef](#)]
13. Rad, M.M.; Ibrahim, S.K. Optimal Plastic Analysis and Design of Pile Foundations Under Reliable Conditions. *Period. Polytech. Civ. Eng.* **2021**, *65*, 761–767. [[CrossRef](#)]
14. Kaliszky, S.; Lógó, J. Optimal plastic limit and shake-down design of bar structures with constraints on plastic deformation. *Eng. Struct.* **1997**, *19*, 19–27. [[CrossRef](#)]
15. Kaliszky, S.; Lógó, J. Optimal strengthening of elasto-plastic trusses with plastic deformation and stability constraints. *Struct. Optim.* **1999**, *18*, 296–299. [[CrossRef](#)]
16. Lógó, J.; Rad, M.M.; Knabel, J.; Tauzowski, P. Reliability based design of frames with limited residual strain energy capacity. *Period. Polytech. Civ. Eng.* **2011**, *55*, 13–20. [[CrossRef](#)]
17. Murzewski, J. *Probability, Reliability and Statistical Methods in Engineering Design*; Halder, A., Mahadevan, S., Eds.; John Wiley & Sons: New York, NY, USA, 2000; p. xi+ 304.
18. Hasofer, A.M. Reliability index and failure probability. *J. Struct. Mech.* **1974**, *3*, 25–27. [[CrossRef](#)]
19. Simulia, D.S. *ABAQUS 2018. User's Manual. Dassault Systems, Analysis User's Guide, Volume IV: Elements*; 2018.
20. Hafezolghorani, M.; Hejazi, F.; Vaghei, R.; Jaafar, M.S.B.; Karimzade, K. Simplified Damage Plasticity Model for Concrete. *Struct. Eng. Int.* **2017**, *27*, 68–78. [[CrossRef](#)]
21. Sumer, Y.; Aktaş, M. Defining parameters for concrete damage plasticity model. *Chall. J. Struct. Mech.* **2015**, *1*, 149–155. [[CrossRef](#)]
22. Vaiana, N.; Capuano, R.; Rosati, L. Evaluation of path-dependent work and internal energy change for hysteretic mechanical systems. *Mech. Syst. Signal Process.* **2023**, *186*, 109862. [[CrossRef](#)]
23. Vaiana, N.; Rosati, L. Classification and unified phenomenological modeling of complex uniaxial rate-independent hysteretic responses. *Mech. Syst. Signal Process.* **2023**, *182*, 109539. [[CrossRef](#)]
24. *BS EN 1990:2002*; Eurocode—Basis of Structural Design. British Standards Institution: Chiswick, UK, 2002.
25. Sessa, S.; Marmo, F.; Vaiana, N.; Rosati, L. Probabilistic assessment of axial force–biaxial bending capacity domains of reinforced concrete sections. *Meccanica* **2019**, *54*, 1451–1469. [[CrossRef](#)]

Disclaimer/Publisher's Note: The statements, opinions and data contained in all publications are solely those of the individual author(s) and contributor(s) and not of MDPI and/or the editor(s). MDPI and/or the editor(s) disclaim responsibility for any injury to people or property resulting from any ideas, methods, instructions or products referred to in the content.